ELSEVIER

Journal of Hydrology 191 (1997) 290–314

Journal of Hydrology

The influence of artificial macropores on water and solute transport in laboratory soil columns

J.M. Buttle[a,*], D.G. Leigh[b]

[a]*Department of Geography, Trent University, Peterborough, Ont., K9J 7B8 Canada*
[b]*Watershed Ecosystems Graduate Program, Trent University, Peterborough, Ont., K9J 7B8 Canada*

Received 14 September 1995; revised 1 February 1996; accepted 2 February 1996

Abstract

The role of macropores in infiltration through a sandy loam was studied using laboratory columns pretreated with water possessing a $\delta^{18}O$ signature of −8.7‰ and 15 mg l^{-1} Cl^-. A simulated snowmelt pulse of $\delta^{18}O$-depleted water containing 1100 mg l^{-1} Cl^- was added to a control column and two columns containing a single vertical macropore, one continuous and the other discontinuous. Macropores were formed in situ by disintegration of a biodegradable foam thread inserted during column packing. Macropores were 2 mm in diameter, which has been suggested to be the threshold for significant macropore flow given the soil's mean textural pore diameter of 0.41 mm. Meltwater was flushed from the columns by adding two pore volumes of isotopically enriched water containing 15 mg l^{-1} Cl^- at a rate of 17.2 mm day^{-1}. Tensiometers, time domain reflectometry probes and suction samplers were used to monitor matric potential, soil water content and soil water chemistry at 0.1 m intervals down the columns. Column effluent was sampled daily for $\delta^{18}O$ and Cl^-. Mobile soil water contents (θ_m) and dispersivities (ϵ) were estimated by fitting a one-dimensional analytical solution of the convection–dispersion equation to Cl^- breakthrough curves (BTCs). θ_m increased with depth in all columns, whereas only the discontinuous macropore column showed an increase in ϵ with flow length. Cl^- and $\delta^{18}O$ breakthrough occurred earlier at all depths in the macropore columns relative to the control, resulting in larger ϵ values for macroporous soil. ϵ for a given flow length tended to be greatest in the discontinuous macropore column, reflecting the role of internal catchment processes. Macropore presence was associated with decreased θ_m during infiltration and bimodal BTCs in column effluent. The threshold ratio of macropore-to-micropore diameters at which macropores exert a detectable influence on water transport must be less than that examined here. © 1997 Elsevier Science B.V.

* Corresponding author.

PII S0022-1694(96)03079-X

1. Introduction

Macropores are relatively large soil pores that may result from biological activity as well as structural cracks and fissures. Water flow via macropores is frequently non-laminar (Chen and Wagenet, 1992), allowing infiltrating water to bypass the soil matrix and reach specific depths faster than water moving through soil micropores. This has two important implications: (1) infiltration is not adequately described by models based on Darcian assumptions (Beven and Germann, 1982; Bouma, 1990); (2) solutes carried by infiltrating water may bypass the matrix (Nielsen et al., 1986), thus reducing soil contact time and the soil's effectiveness as a solute source or sink.

There have been four general approaches to the study of macropores and their influence on water and solute transport in soils:

1. Field studies using hydrometric methods and/or natural and artificial tracers (e.g. Jardine et al., 1989; Sophocleous et al., 1990). These permit assessment of macropore flow under field conditions; nevertheless, they face the complexities introduced by climatic variability, as well as difficulties associated with assessment of hydraulic properties in the field.
2. Laboratory studies with intact soil (e.g. Elrick and French, 1966; Edwards et al., 1993). This approach permits an intact soil section to be analysed under controlled conditions. However, as with field studies, it is often difficult to distinguish macropore effects from those introduced by the inherent complexity of natural soil systems. There are often no a priori data on the internal composition of the extracted soil (Flury et al., 1994), and it may not be possible to simulate unsaturated flow conditions adequately using the extracted soil (Tindall et al., 1992).
3. Modelling studies (e.g. Germann and Beven, 1986; Jarvis et al., 1991; Booltink, 1994). Models facilitate study of climatic and pedologic controls on macropore flow. A major limitation facing the application of models to field conditions is the accurate quantification of parameters which control bypass flow via macropores, such as pore continuity and the rate of water supply to the macropore relative to the hydraulic conductivity of the soil matrix.
4. Laboratory studies with artificial macropores (e.g. Bouma and Anderson, 1977; Czapar et al., 1992; Stehouwer et al., 1994). These involve the creation of a macropore of known dimensions in a standardized soil. Although highly artificial, use of a standardized artificial soil eliminates the influence of textural and structural variations on the soil's physical behaviour, and permits study of the effect of individual macropore properties on soil physicochemical behaviour (Bouma and Anderson, 1977).

This paper describes a new method of creating artificial macropores in laboratory soil columns. It also examines the influence of continuous and discontinuous macropores of known dimensions on the hydraulic properties of a standardized soil.

2. Materials and methods

2.1. Columns

Three 0.5 m × 0.5 m × 0.65 m stainless steel columns (Fig. 1) were used. The perforated

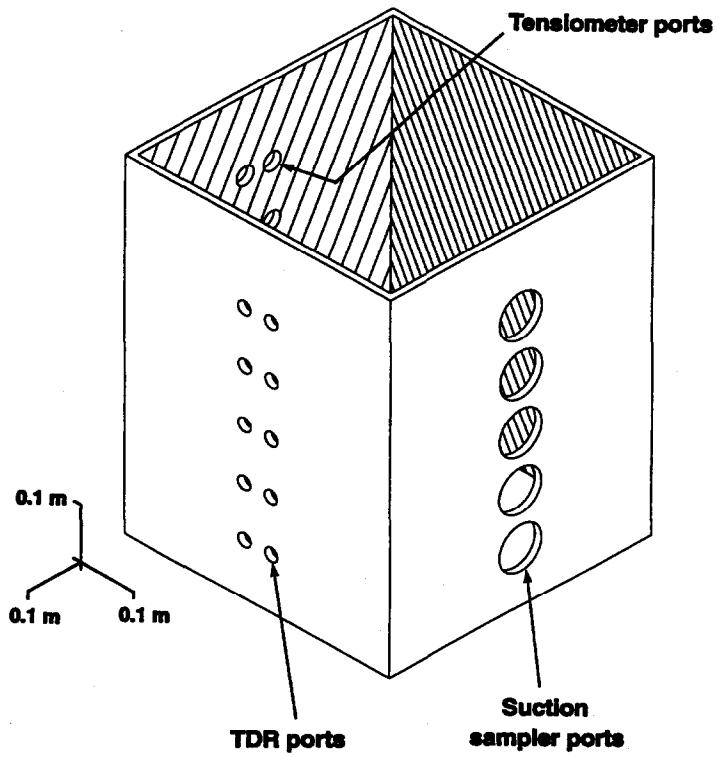

Fig. 1. Schematic diagram of soil column, showing location of access ports for TDR probes, tensiometers and suction samplers.

base of each column was covered with sheets of steel mesh and Nytex to prevent loss of fine material during packing and experimentation. Before packing, the interior walls of the columns were coated with a thin layer of silicone to seal soil to the column walls and thus minimize boundary flow. Columns were packed to a depth of 0.6 m with air-dried homogenized sandy loam (43% sand, 50% silt, 7% clay; mean grain size, 0.41 mm; standard deviation, 0.37 mm), with a uniform bulk density of 1300 kg m^{-3} and mean saturated hydraulic conductivity (K_H) of $2.3 \times 10^{-7} \pm 0.3 \times 10^{-7}$ m s^{-1}. This is within the range of K_H for fine and silty sands (Fetter, 1994).

A control column (Column A) was compared with columns containing continuous (Column B) and discontinuous (Column C) macropores. The macropores were created by inserting a vertical thread of biodegradable foam (2 mm diameter) in the centre of the column during packing. The thread was positioned above one of the perforations in the column base. The foam breaks down upon wetting, such that column pretreatment was expected to produce a macropore of 2 mm diameter in situ. According to a relation presented by Kirkby (1988), this represents the critical macropore diameter required to produce significant bypassing flow for a textural pore size of 0.41 mm (assumed to be equivalent to the mean grain diameter; Fig. 2). The continuous macropore in Column B was 0.6 m in length, whereas a break in the foam thread of 0.1 m thickness between

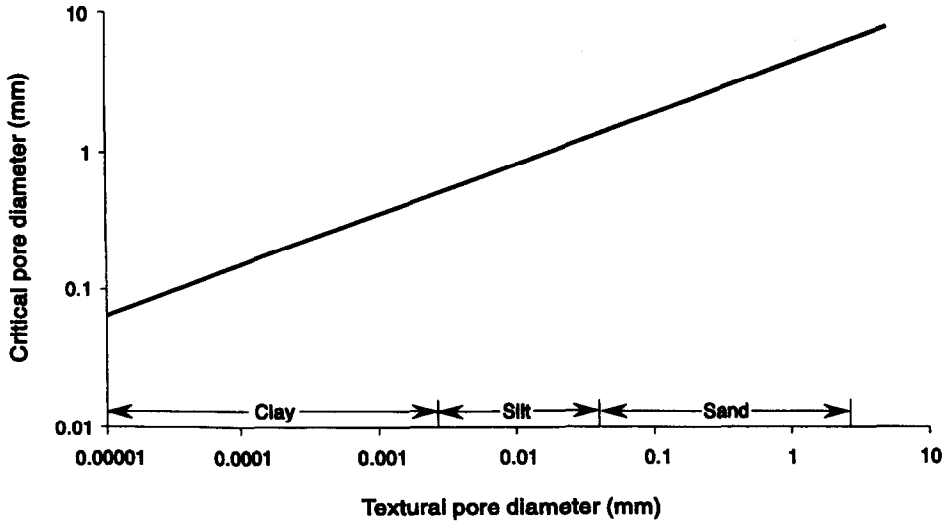

Fig. 2. Critical minimum macropore diameter that will allow bypassing for a given pore (grain) diameter of the soil matrix. After Kirkby (1988) and Dingman (1993).

0.25 and 0.35 m below the soil surface in Column C resulted in a discontinuous macropore.

A suction sampler, two time domain reflectometry (TDR) probes, and two tensiometers were installed every 0.1 m below the soil surface in all three columns. Suction sampler bulbs were of 5.5 cm length with midpoints located 22.25 cm from the column centre. A suction of 50 kPa was applied, such that water held in macro-, meso- and large micropores was sampled (Luxmoore, 1981). Tensiometer bulbs were of 3 cm length with midpoints located 3.9 and 15.2 cm from the column centre. Each tensiometer was connected to a pressure transducer, and matric potential (ψ) was recorded continuously on a Campbell 21X data logger (Campbell Scientific, Logan, UT, USA). The tensiometer array permitted monitoring of vertical and lateral hydraulic gradients in the columns. Volumetric water content (θ) was measured using a Trase© TDR system (Soilmoisture Equipment, Santa Barbara, CA, USA. The columns drained to a collecting tray. A small plastic funnel was attached to the underside of the base of Columns B and C, directly beneath the perforation draining the artificial macropore. The funnel drained to a 150 ml flask, so that any direct flow from the macropore could be sampled. The column base was wrapped with polyethylene and a polyethylene cover was placed on each column between water applications to minimize evaporation.

2.2. Sampling and analysis

Five measurements of θ were taken twice daily (10:00 h and 16:00 h, EST) at each depth. Samples from all suction samplers and column effluent were collected daily, and aliquots were taken for Cl^- and ^{18}O analysis. The former is often assumed to behave conservatively in soil, and has been frequently used as a tracer in solute transport studies (e.g. Czapar et al., 1992; Munyankusi et al., 1994). Oxygen-18 is not subject to chemical

reactions in soil (Drever, 1988), and was used as a check on Cl^- concentrations to assess whether anion exclusion or adsorption was occurring (McMahon and Thomas, 1974). Cl^- was determined by a specific ion electrode, with a detection limit of 0.001 mg l^{-1} and a precision of ±2%. Oxygen-18 contents were analysed at the University of Waterloo Environmental Isotope Laboratory by mass spectrometry, and reported as the relative deviation of the isotope ratio ($^{18}O/^{16}O$) from that of Standard Mean Ocean Water (SMOW). Analytical accuracy of $\delta^{18}O$ results was ±0.1‰.

2.3. Treatment

Each column was pretreated with three pore volumes (p.v.s) of water with $\delta^{18}O$ of −8.7‰ and 15 mg l^{-1} Cl^-. Pretreatment raised θ in each column to near-saturation (mean θ of 0.45 m^3 m^{-3} ±0.01 m^3 m^{-3}) and allowed dissolution of the foam thread. Drainage from the perforation underlying the foam thread was observed during pretreatment, indicating that dissolution of the foam resulted in a macropore capable of conducting flow. A 10 day simulated snowmelt pulse was then applied at 17.2 mm day^{-1}. Meltwater was at 5°C with a Cl^- concentration of 1100 mg l^{-1}. The $\delta^{18}O$ signature of the meltwater was −17.52‰, −19.75‰ and −18.22‰ for Columns A, B and C, respectively. Water was applied evenly to the soil surface through a perforated Plexiglas tray at the following times and amounts: 10:00 h, 4.3 mm; 13:00 h, 8.6 mm; 16:00 h, 4.3 mm. Applications were made over 15 min (4.3 mm) or 30 min (8.6 mm) intervals, giving a specific flux (q) of 4.8×10^{-6} m s^{-1} during these periods. Water ponded on the soil surface during application and for several minutes following application. Inputs were a crude analogue of continuous water supply to the soil during a typical diurnal snowmelt pulse

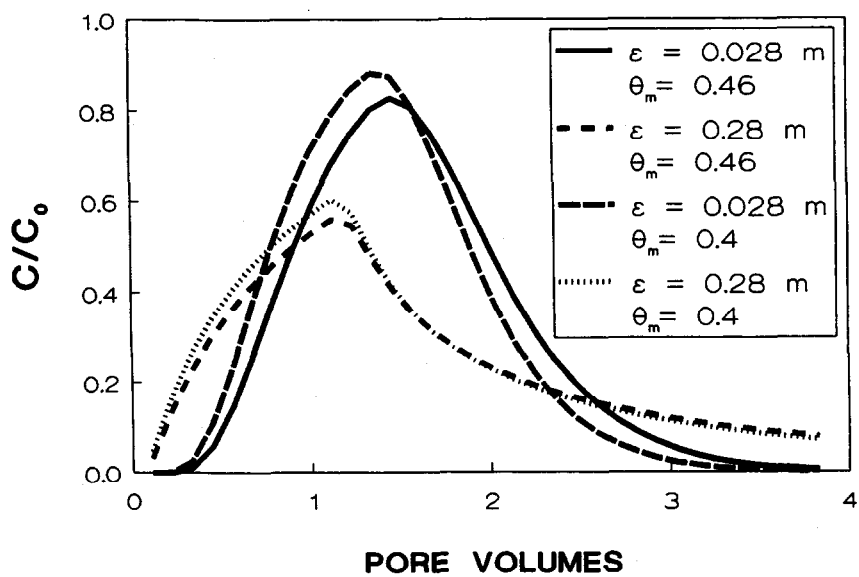

Fig. 3. The influence of changes in dispersivity (ϵ) and mobile soil water content (θ_m) on BTC shape.

in the field; however, this method was adopted to minimize exposure of the input water to the atmosphere and any consequent evaporative enrichment of the $\delta^{18}O$ signature of the infiltrating water. Meltwater was flushed from the columns by adding two p.v.s of water at 17.2 mm day^{-1} using the same application procedure. The water had 15 mg l^{-1} Cl^- and a temperature of approximately 22°C. The $\delta^{18}O$ of this isotopically enriched water was −7.75‰, −8.9‰ and −9.09‰ for Columns A, B and C, respectively, and was intended to approximate the isotopic signature of spring rainfalls.

2.4. Modelling Cl^- BTCs

We hypothesized that macropore presence results in a decrease in mobile soil water content (water that participates in flow during infiltration) and an increase in soil dispersivity (a characteristic property of the medium that quantifies mechanical dispersion), and that these effects will produce BTCs that differ from those observed for a nonmacroporous soil (Fig. 3). Mobile water content and dispersivity were estimated by comparing Cl^- breakthrough curves (BTCs) for suction samplers and column effluent with predictions from an analytical solution of the convection–dispersion equation (CDE) for solute transport (Rose et al., 1982). The model predicts the BTC resulting from pulse-type displacement of a reactive or non-reactive solute in unsaturated soil as

$$\frac{C}{C_0}=0.5\left\{\operatorname{erfc}\left[\frac{z-\alpha}{2(D_0t+\epsilon\alpha)^{0.5}}\right]-\operatorname{erfc}\left[\frac{z-\beta}{2(D_0t+\epsilon\beta)^{0.5}}\right]\right\} \tag{1}$$

where C is the Cl^- concentration (mg l^{-1}) at depth z and time t minus background Cl^- concentration; C_0 is the Cl^- concentration in the feed water (1100 mg l^{-1}) minus background Cl^- concentration; α is the mean Cl^- penetration depth (m), which equals $I/(\theta_m R)$ (where I is the total amount of water infiltrated (m), θ_m is the average volumetric content of mobile water above depth z, and R is the retardation factor); D_0 is the Cl^- diffusion coefficient ($m^2\ s^{-1}$); ϵ is the dispersivity (m); β is the water penetration depth (m), which equals $\alpha - \Delta F$; ΔF is the thickness of applied Cl^- pulse (m), which equals the depth equivalent of the applied snowmelt pulse (0.172 m) divided by θ_m; t is time (s).

Water input was 0.0172 m day^{-1}, R was unity, and D_0 was 1.6×10^{-9} $m^2\ s^{-1}$. θ_m and ϵ values that produced the best goodness-of-fit between observed and predicted BTCs were obtained by maximizing the model efficiency (EFF):

$$\mathrm{EFF}=\frac{\left[\sum_{i=1}^{n}(O_i-\bar{O})^2-\sum_{i=1}^{n}(O_i-P_i)^2\right]}{\sum_{i=1}^{n}(O_i-\bar{O})^2}\times 10 \tag{2}$$

where O_i is the observed value at time period i, $\bar{O}$ is the mean of the observed values, P_i is the predicted value at time period i, and n is the number of time periods.

Standard errors associated with the water and Cl^- balances for the columns were approximated by the probable error associated with the sum or difference of the independent variables, or with their product or quotient (Davidson, 1978). Assumed fractional errors for each balance component have been given by Leigh (1995).

3. Results and discussion

3.1. Hydraulic conditions and column water balance

Initiation of macropore flow occurs when specific flux exceeds infiltration into the topsoil matrix (Beven and Germann, 1982; Booltink, 1994), and q during application exceeds the soil's K_H by an order of magnitude. Assuming that the latter approximates

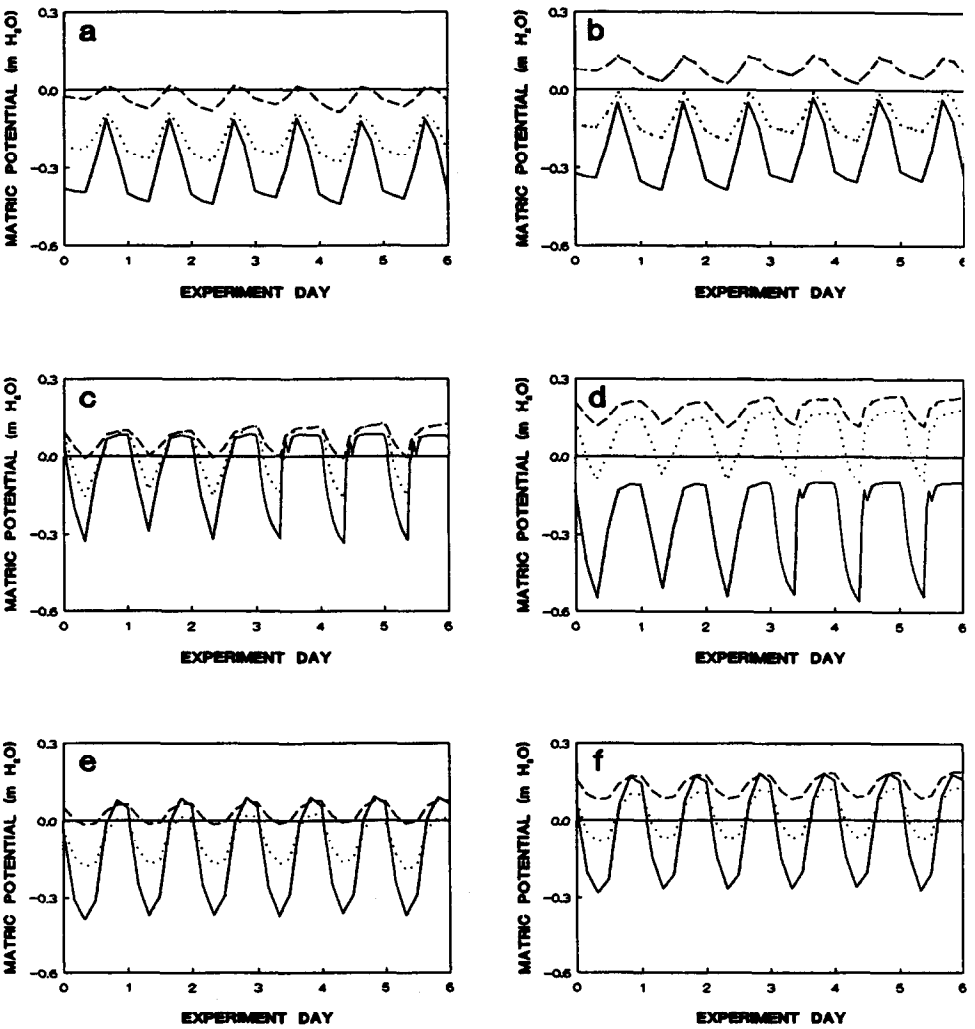

Fig. 4. Temporal trends in matric potential (ψ) at various depths (continuous line, 0.1 m; dotted line, 0.3 m; dashed line, 0.5 m) for a 6 day period in the experiment: (a) Column A matrix; (b) Column A matrix near the column centre; (c) Column B matrix; (d) Column B matrix near the column centre; (e) Column C matrix; (f) Column C matrix near the column centre.

Table 1
Column water balances (±1 standard error); depths are expressed relative to the column surface area (0.25 m^2)

Water balance component	Column A	Column B	Column C
Input (mm)	886	757.3	916.5
	(12.4)	(10.6)	(12.8)
Outputs (mm)			
Suction samplers	101.7	112.1	104.8
	(1.4)	(1.6)	(1.5)
Column effluent	768.9	596.2	741.7
(macropore effluent not included)	(10.8)	(8.3)	(10.4)
Macropore effluent	–	1.1	0.2
		(1.5×10^{-2})	(2.8×10^{-3})
ΔStorage (mm)	− 25.3	− 17.4	0.7
	(5.5)	(4.5)	(0.2)
(Outputs + ΔStorage)/Input	0.959	0.961	0.984
	(0.013)	(0.013)	(0.014)

matrix infiltration, it appears that macropore flow could be initiated during water application to the columns. Peak snowmelt rates in the field can exceed 1.1×10^{-6} m s^{-1} (Buttle, 1989), suggesting that macropore flow could also occur under more natural inputs to this soil.

Water inputs induced consistent diurnal wetting and draining in all columns (Fig. 4), such that ψ responses to the intermittent meltwater additions were similar to those observed during snowmelt in the field (e.g. Buttle, 1989). Fig. 5 shows total potential (Φ) patterns in column cross-sections 7 days after the start of the experiment, shortly after water application. These patterns are representative of hydraulic conditions observed following application throughout the experiment, owing to the consistent temporal trends in ψ (Fig. 4). The control column showed weak lateral hydraulic gradients towards the column walls during drainage, and strong downward hydraulic gradients in the upper column immediately following water application. In contrast, both macropore columns had higher Φ at a given depth and relatively greater vertical and lateral hydraulic gradients directed away from the column centre, particularly during drainage. Although these Φ patterns were not as definitive as those presented elsewhere (e.g. Edwards et al., 1979), they suggest radial flow away from the macropore and greater vertical movement of the wetting front relative to infiltration in a nonmacroporous soil.

Column water balances (Table 1) indicated that 96–98% of water applied to the columns could be accounted for by extraction by suction samplers, column effluent and change in storage. Evaporation was therefore considered to be minimal during the experiment, and Cl^- concentrations in suction samples and effluent did not require correction. Despite the influence of macropores on hydraulic conditions within Columns B and C, total direct drainage via the macropores was small. Continuous macropores have been reported to be more important vectors of water and solutes than discontinuous pores (e.g. Quisenberry and Phillips, 1978; Tippkotter, 1983), and this was supported by the larger total flux from the continuous macropore (Table 1).

Daily column effluent was divided by the total number of perforations in the column

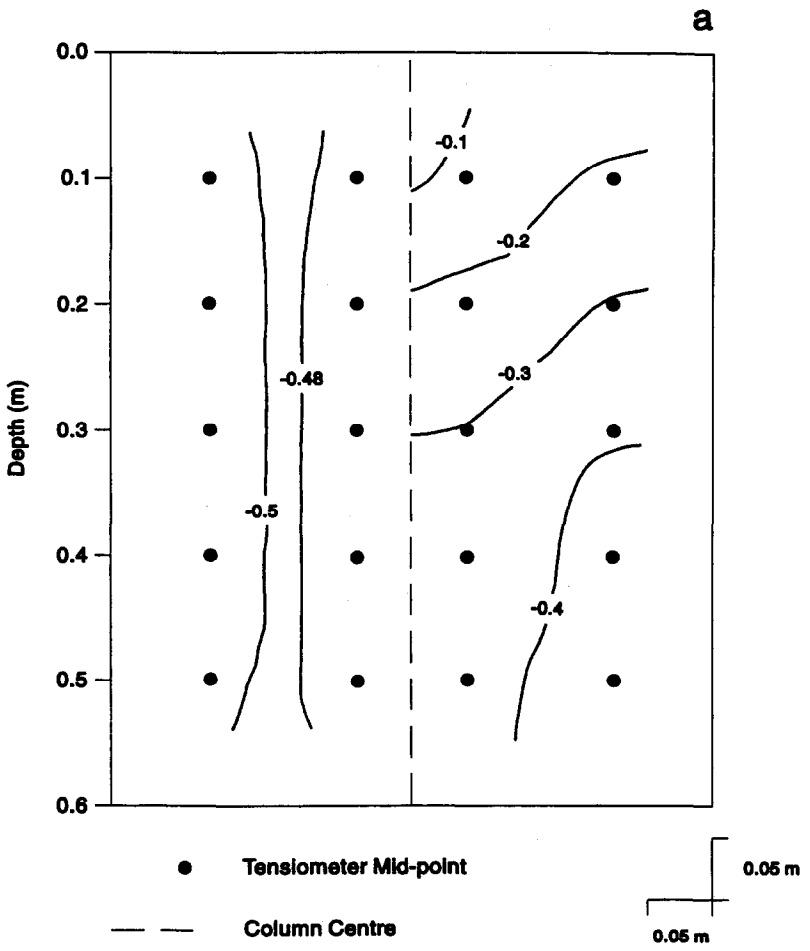

Fig. 5. Cross-section of control (a) and macropore columns ((b) and (c)) 7 days after the start of the experiment, showing the two-dimensional pattern of total potential (Φ) in the soil matrix between the centre of the column and the column wall. ●, Tensiometer mid-points. The left-hand side of each cross-section indicates Φ during drainage, and the right-hand side shows the pattern of Φ immediately after water application at the column surface. The question mark at the end of the 0 m equipotential for the continuous macropore column (b) reflects potentially inaccurate ψ data from the 0.1 m tensiometer near the column centre.

base to obtain the mean flux per perforation. This was compared with the daily macropore effluent (Fig. 6). Drainage via the continuous macropore in Column B was initially greater than that from the surrounding matrix, although this difference decreased over time. In contrast, drainage from the discontinuous macropore was consistently lower than the mean flux per perforation, suggesting that the continuous macropore was relatively more effective in promoting bypassing flow, particularly during the initial stage of the experiment. However, a more pronounced difference in flow from the continuous and discontinuous macropores may not have been observed owing to the use of a daily timestep. This did not

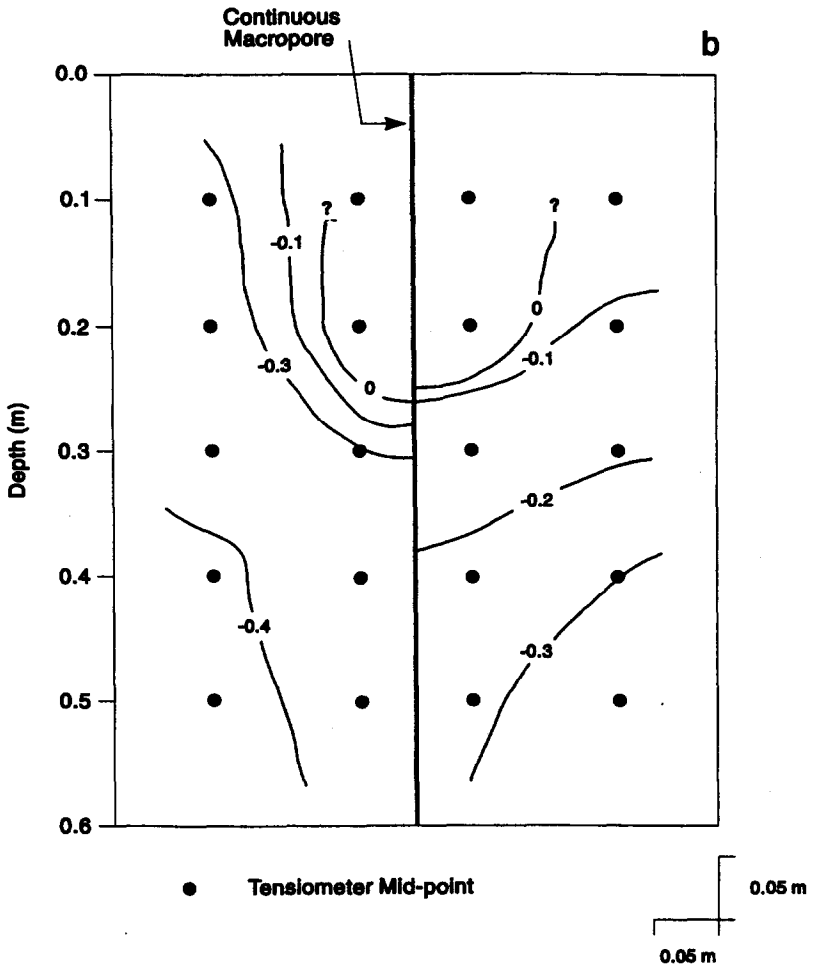

Fig. 5. Continued.

permit detection of enhanced flow expected to arise from presence of a continuous macropore, which may only occur within minutes or hours of water application at the column surface (cf. Edwards et al., 1979). It is also unlikely that all macropore flow left the column through the funnel; instead, much of the water conveyed to the column base via the macropore was probably incorporated into the saturated layer that formed at the column base and contributed to total column drainage.

3.2. Cl^- and $\delta^{18}O$ breakthrough

BTCs of Cl^- and $\delta^{18}O$ (Fig. 7) indicate infiltration of Cl^--rich meltwater, followed by passage of ^{18}O-enriched, Cl^--depleted water. The 0.5 m suction sampler in Column B did not provide sufficient sample for ^{18}O analysis later in the experiment, resulting in an

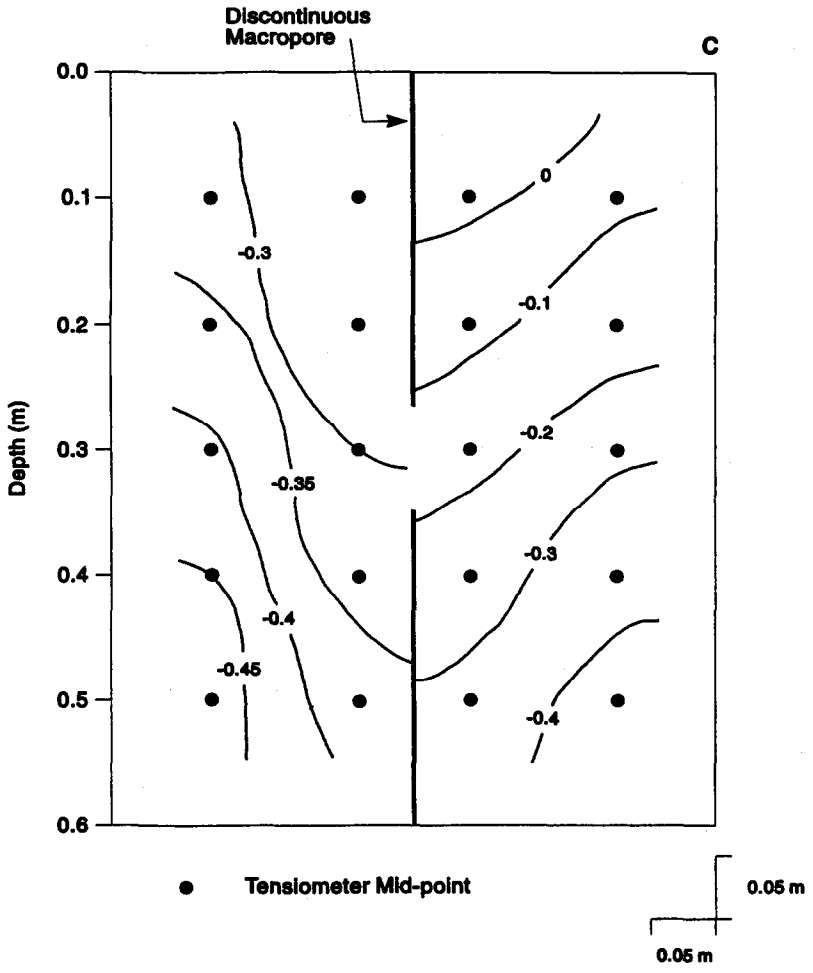

Fig. 5. Continued.

incomplete $\delta^{18}O$ BTC (Fig. 7(e)). Cl^- and ^{18}O BTCs were similar, suggesting that anion exclusion and Cl^- adsorption were insignificant (cf. McMahon and Thomas, 1974). Cl^- mass balances (Table 2) show that approximately 100% of applied Cl^- was accounted for. Therefore Cl^- was assumed to be conservative, and subsequent analyses are restricted to the more detailed Cl^- BTCs.

Peak C/C_0 values were similar for all columns at the 0.1–0.4 m depths, with smaller peak C/C_0 values at greater depths in the macropore columns. Suction sampler and effluent BTCs for Column A were highly symmetrical compared with the macropore columns. BTCs for Column B exhibited more protracted rising limbs with depth, whereas BTC falling limbs for Column C became more extended with depth. Effluent BTCs for the macropore columns were slightly bimodal. Asymmetrical and bimodal BTCs may reflect

Table 2
Column Cl^- mass balances (±1 standard error)

Mass balance component	Column A	Column B	Column C
Input (g)	50.1	49.6	50.2
	(2.9)	(2.8)	(2.9)
Outputs (g)			
Suction samplers	7.3	8.4	7.3
	(0.4)	(0.5)	(0.4)
Column effluent	46.2	42.0	43.8
(macropore effluent not included)	(2.6)	(2.4)	(2.5)
Macropore effluent	–	0.0	0.0
		(2.3×10^{-3})	(1.7×10^{-4})
ΔStorage (g)	−0.1	−0.1	0.0
	(2.1×10^{-2})	(1.8×10^{-2})	(1.8×10^{-2})
(Outputs + ΔStorage)/Input	1.066	1.019	1.021
	(0.031)	(0.029)	(0.03)

diffusion of Cl^- from active to inactive pores during meltwater flux through the soil (Van Stiphout et al., 1987; Jarvis et al., 1991) followed by Cl^- release to the subsequent passage of dilute water, thus raising concentrations above input levels.

The Cl^- pulse appeared earlier in the macropore columns relative to Column A at all depths (Fig. 7, Table 3). Similar results were found in BTC comparisons for disturbed and undisturbed (i.e. macroporous) soil cores (e.g. Elrick and French, 1966), and for columns with and without artificial macropores (e.g. Bouma and Anderson, 1977; Czapar et al., 1992). Paired *t*-tests indicated that p.v.s required to reach Cl^- $C/C_0 = 0.3$ at a given depth in the macropore columns were significantly smaller ($P = 0.05$) than for the control. In turn, p.v.s at $C/C_0 = 0.3$ were lower for Column C relative to Column B ($P = 0.05$). Macropores

Table 3
Pore volumes required to reach specified Cl^- C/C_0 values at various depths

Depth (m)	Column A	Column B	Column C
Pore volumes at $C/C_0 = 0.3$			
0.1	0.87	0.73	0.69
0.2	0.82	0.69	0.53
0.3	0.90	0.56	0.49
0.4	0.91	0.69	0.58
0.5	0.97	0.76	0.65
0.6[a]	0.7	0.53	0.56
Pore volumes at $C/C_0 = 0.5$			
0.1	1.12	0.93	0.88
0.2	1.24	0.94	0.72
0.3	1.13	0.75	0.66
0.4	1.14	1.22	0.73
0.5	1.17	1.40	0.80
0.6[a]	0.86	0.79	0.76

[a] Not included in statistical testing.

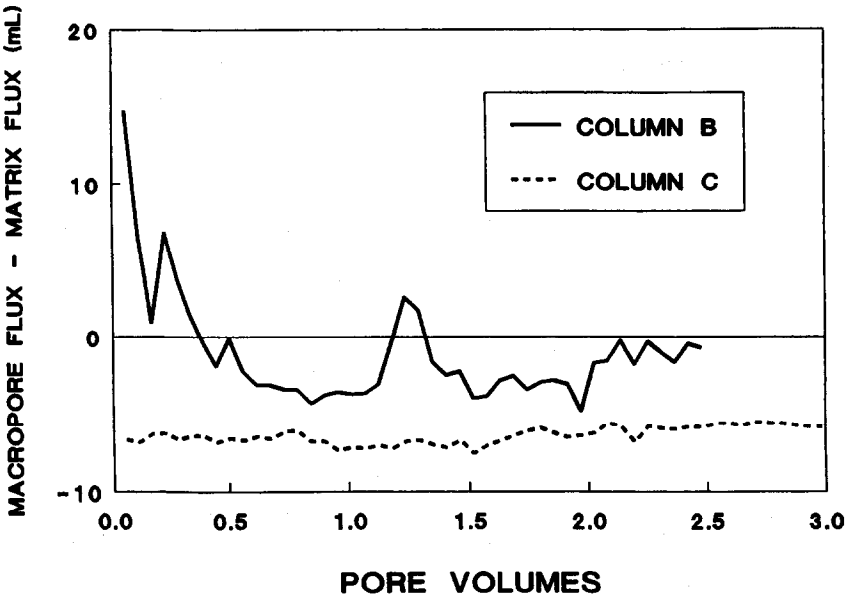

Fig. 6. Difference in daily drainage between the macropore and the mean flux per perforation for the surrounding soil matrix.

in Columns B and C allowed suction samplers at a given depth to obtain Cl^--rich water before samplers in Column A, probably as a result of radial flux of tracer away from the macropore. There was no significant difference in p.v.s needed to obtain Cl^- $C/C_0 = 0.5$ for Columns A and B or Columns C and B; however, p.v.s at $C/C_0 = 0.5$ were significantly lower for Column C relative to Column A. Earlier Cl^- breakthrough for Column C may reflect a more efficient and/or well-defined pore in the upper 0.2 m relative to Column B. It may also be a function of enhanced entry of Cl^- into the matrix as a result of the 0.1 m break in the macropore, which may have slowed vertical transport of the tracer and promoted lateral movement into the surrounding soil (the internal catchment process described by Van Stiphout et al. (1987)). Thus, relatively more Cl^- was introduced to the matrix at depth compared with Column B. Column effluent values (0.6 m depth) were obtained by a different sampling method and were not included in the paired *t*-tests; nevertheless, p.v.s associated with C/C_0 values of 0.3 and 0.5 in macropore column effluent were smaller than for the control.

Results indicate that the macropores served as preferential flow paths; however, they did not exhibit pronounced differences in breakthrough times between macroporous and non-macroporous soil reported elsewhere (e.g. Bouma and Anderson, 1977; Czapar et al., 1992). This may reflect the relatively low application rate (0.0172 m day^{-1}) compared with other studies: 0.027 m day^{-1} used by De Smedt et al. (1986), 0.043 m day^{-1} used by Smettem (1984), and 0.060 m day^{-1} used by Shipitalo et al. (1990). Higher application rates favour more rapid preferential flow and consequently faster tracer breakthrough (cf. Smettem, 1984; Bouma, 1990; Edwards et al., 1993). Our low application rate may have

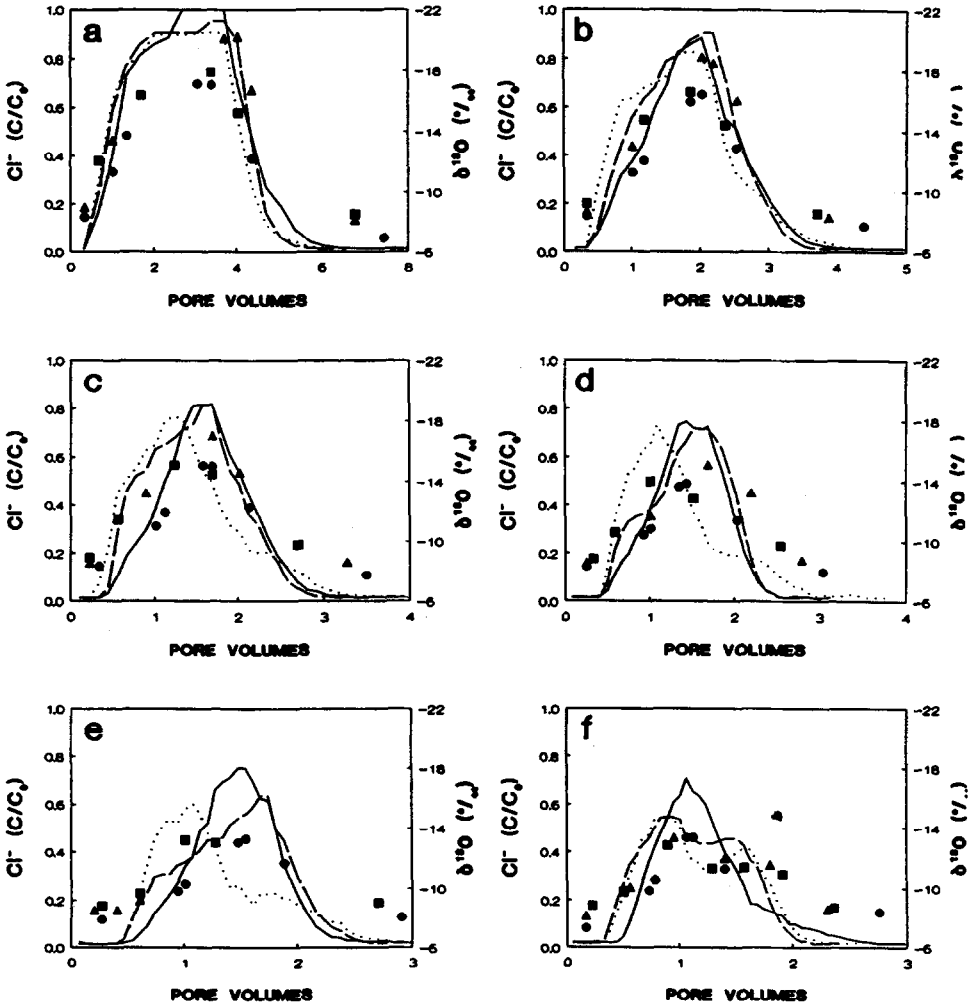

Fig. 7. BTCs for control column (continuous line, Cl^- C/C_0; ●, $\delta^{18}O$), continuous (dashed line, Cl^- C/C_0; ▲, $\delta^{18}O$) and discontinuous (dotted line, Cl^- C/C_0; ■, $\delta^{18}O$) macropore columns: (a) 0.1 m suction sampler; (b) 0.2 m suction sampler; (c) 0.3 m suction sampler; (d) 0.4 m suction sampler; (e) 0.5 m suction sampler; (f) column effluent. BTCs are plotted against pore volumes of applied water, where the pore volume for a particular sample depth is the product of porosity and distance from the soil surface.

allowed greater mixing with matrix water and more mobile–immobile water exchange than would occur under higher rates (Van Stiphout et al., 1987). In addition, the earlier studies used soils with macroporosities (defined by Chen and Wagenet (1992) as the ratio of macropore cross-sectional area to total soil cross-sectional area) ranging from 2.6×10^{-2} (Jones et al., 1993) to 1.4×10^{-4} (Anderson et al., 1990)—much greater than the 1.3×10^{-5} used here. Greater macroporosity combined with similar or larger application rates may have produced breakthrough times comparable with those from previous work.

Table 4
Model efficiencies (EFF), mobile soil water contents (θ_m), dispersivities (ϵ) and Peclet numbers (P) obtained in fitting the Rose et al. (1982) model (Eq. (1)) to Cl^- BTCs observed at depth z

z (m)	Column A				Column B				Column C			
	EFF (%)	θ_m ($m^3\ m^{-3}$)	ϵ (mm)	P	EFF (%)	θ_m ($m^3\ m^{-3}$)	ϵ (mm)	P	EFF (%)	θ_m ($m^3\ m^{-3}$)	ϵ (mm)	P
0.1	99.9	0.35	22	4.0	99.9	0.30	19	4.7	99.9	0.23	44	2.2
0.2	99.8	0.42	46	4.1	99.9	0.38	32	5.7	99.9	0.30	86	2.3
0.3	99.9	0.46	28	9.5	99.8	0.38	46	6.1	99.9	0.30	125	2.4
0.4	99.8	0.50	20	16.7	99.9	0.44	45	8.2	100.0	0.35	100	3.9
0.5	99.9	0.54	13	28.8	99.5	0.55	37	12.1	99.8	0.40	110	4.4
0.6[a]	99.9	0.41	45	12.4	99.6	0.38	91	6.4	99.6	0.38	115	5.1

[a] Not included in statistical testing.

3.3. Modelling Cl^- BTCs

Optimization of Eq. (1) provided excellent fits to observed BTCs (Fig. 8), with all model efficiencies (Eq. (2)) exceeding 99%. Derived θ_m and ϵ values are presented in Table 4. The CDE was least successful at fitting the bimodal effluent BTCs, as noted in other studies (e.g. Beven and Young, 1988). Caution must be exercised in attaching any physical significance to θ_m and ϵ values. Beven and Young (1988) noted that parameter values obtained from fitting the CDE to BTCs may be highly intercorrelated, implying that these parameters are ill-defined and therefore not physically meaningful. However, there was no significant correlation ($P = 0.1$) between θ_m and ϵ values obtained for each column using fits to suction sampler BTCs. Of greater concern are the Peclet (P) numbers for the columns. The Peclet number is a measure of the relative importance of convective and dispersive processes in the columns, and is defined as

$$P = \frac{vL}{D} \tag{3}$$

where v is the mean pore water velocity ($m\ s^{-1}$), which is taken as the solution flux ($m\ s^{-1}$) divided by θ_m at a given L; L is length (m); D is the coefficient of hydrodynamic dispersion, which equals $\epsilon v + D_0$.

The columns had Peclet numbers less than 32 at all depths (Table 4), which Germann (1991) demonstrated was the threshold required for full dispersion of a solute and thus appropriate application of the CDE. Small P values are a common problem in tracer studies using small columns (cf. Kluitenberg and Horton, 1990), and derived θ_m and ϵ values cannot be used to predict flow and transport in larger systems. However, the values still provide characterizations of the transport properties of the columns (Kluitenberg and Horton, 1990), and comparisons of θ_m and ϵ between columns may be valid.

Paired t-tests on suction sampler BTCs indicated smaller θ_m values in the macropore columns relative to the control ($P = 0.05$). In turn, θ_m was lower for Column C relative to Column B ($P = 0.05$). Thus, the proportion of immobile water (θ_{im}), or water not actively involved in flow owing to the reduced participation of matrix water, increased from Column A to B to C. Greater θ_{im} in macroporous vs. nonmacroporous soil was noted in

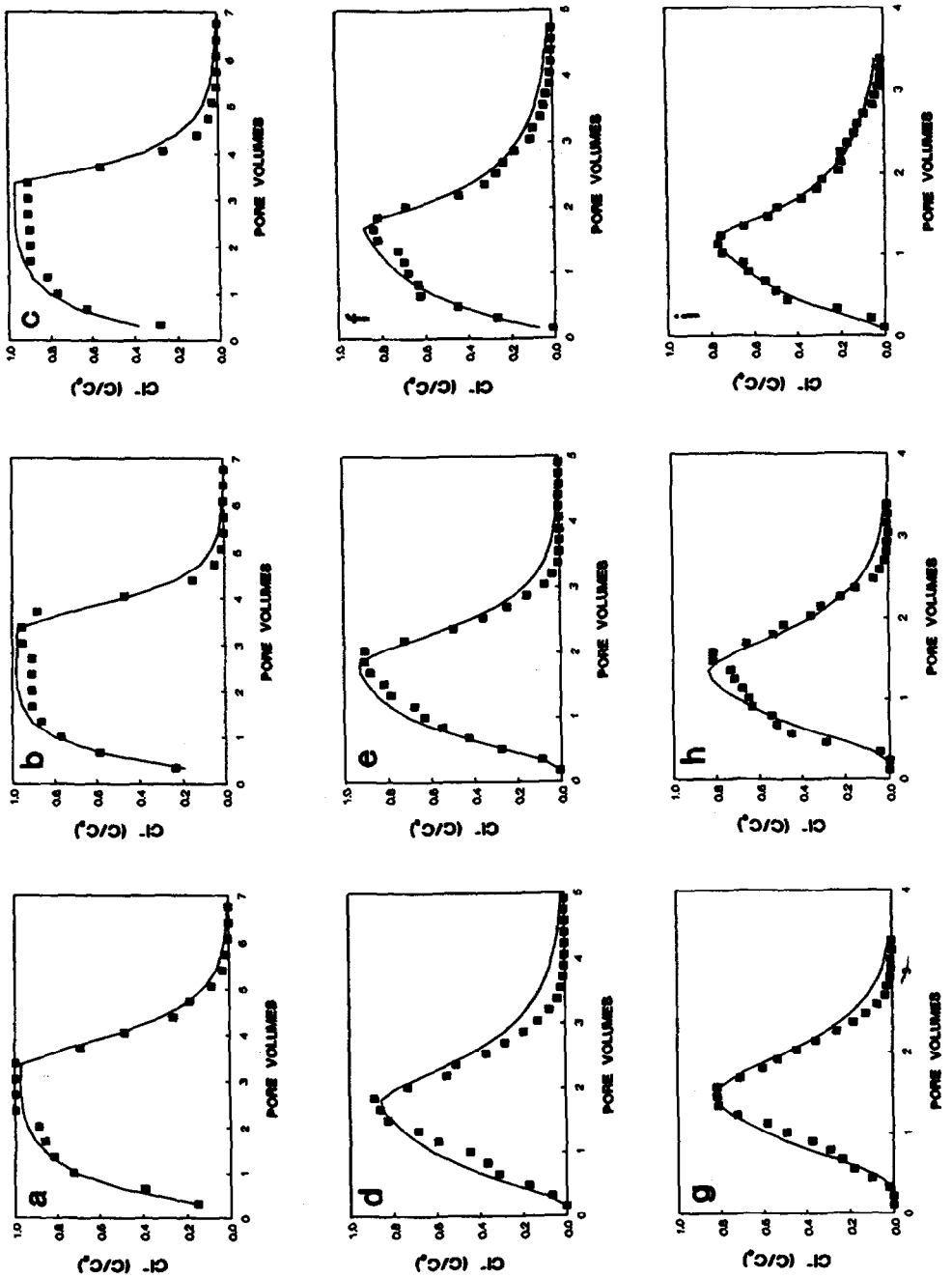
a
b
c
d
e
f
g
h
i
Cl⁻ (C/C₀)
PORE VOLUMES

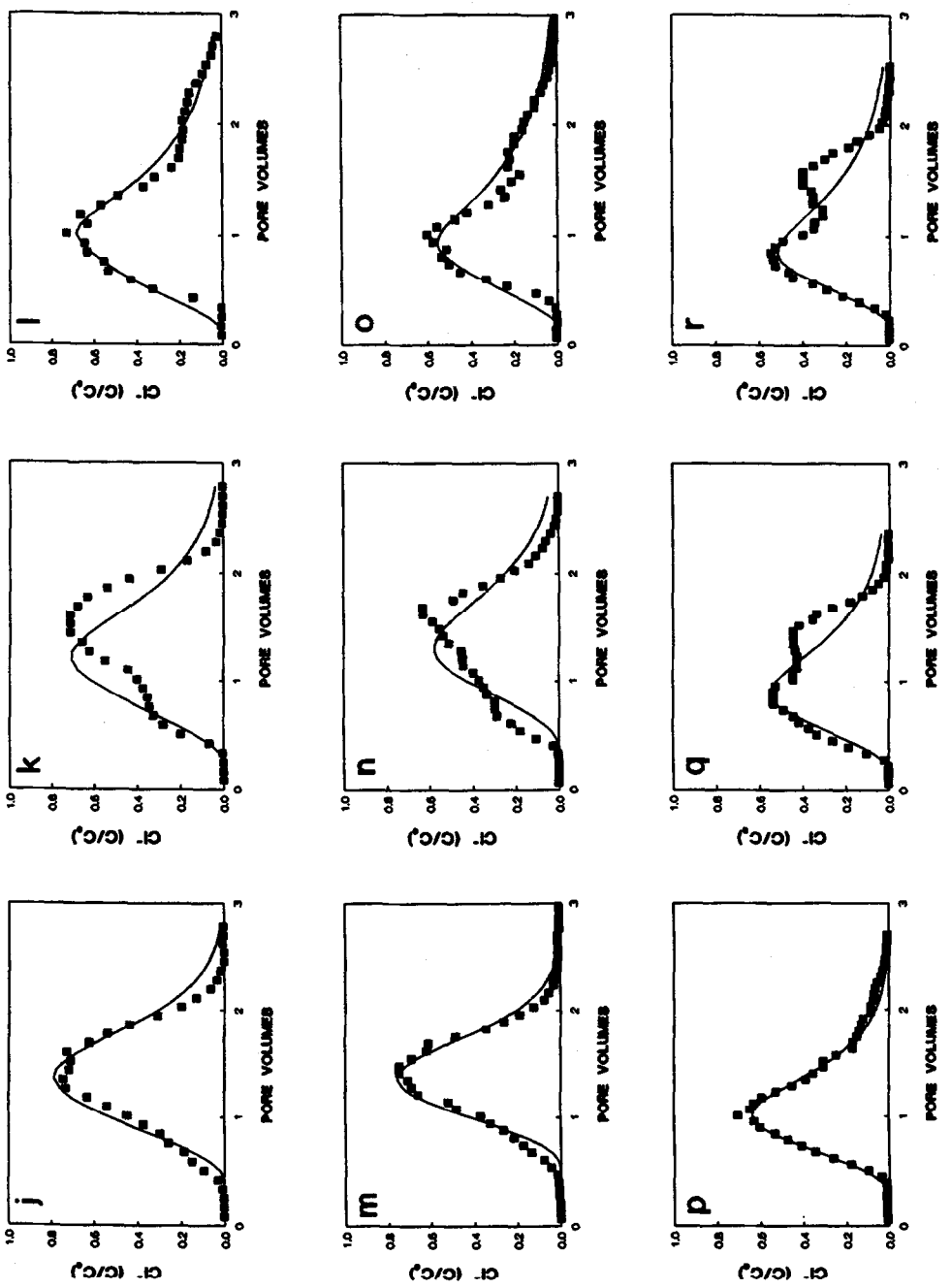
l
o
r
k
n
q
j
m
p
Cl⁻ (C/C₀)
PORE VOLUMES

studies using undisturbed soil columns (e.g. De Smedt et al., 1986) and artificial macropores (Bouma and Anderson, 1977). This has implications for water sampling in macroporous soils. Suction samplers used under large tensions may detect solute presence faster than if macropores are not present; however, they may also obtain water from pores that do not participate in flow. Increased θ_{im} in macroporous soil will result in suction samplers removing some water that is not chemically representative of that moving through the soil, and underestimation of solute concentrations in infiltrating water. This is consistent with smaller peak C/C_0 values for deeper suction samplers in the macropore columns relative to Column A.

Dispersivity was positively correlated with flow length ($r = 0.75$, $P = 0.05$) for Column C, but was not associated with flow length in the other columns (Table 4). Lack of correlation between ϵ and z supports the homogeneity of the soil system in Column A, and suggests that the influence of the continuous macropore upon solute dispersion in Column B was relatively consistent with depth. The significant correlation observed for Column C may reflect the discontinuity in the macropore, which disrupts flow from 0.25 m below the surface to the column's base. The heterogeneity of Column C appears more representative of field situations, where ϵ has been found to increase with flow length (Neuman, 1990).

Paired t-tests revealed that ϵ values were significantly larger for the macropore columns relative to Column A ($P = 0.05$), and were larger in Column C than in Column B. Thus, macropore presence resulted in a significant increase in soil dispersivity. De Smedt et al. (1986) and Smettem (1984) attributed the relatively greater ϵ in macroporous soil to a decreased drained porosity and thus enhanced mobile–immobile exchange during unsaturated flow. Larger ϵ values observed for Column C may reflect the greater heterogeneity of this soil system owing to the macropore discontinuity, subsequent internal catchment processes, and increased exchange of tracer between mobile and immobile water regions.

Column effluent values (0.6 m depth) were not included in the statistical tests, as they were obtained by a different sampling method; nevertheless, they also indicate a smaller θ_m and larger ϵ for the macropore columns relative to Column A.

3.4. Conceptual flow models for the three columns

Fig. 9 summarizes flow processes for the columns. Schematic cross-sections indicate hypothesized vertical and lateral variations in Cl^- C/C_0 when peak C/C_0 was observed at the various sampling depths, the occurrence of which is shown relative to the effluent BTC.

Solute transport in Column A (Fig. 9(a)) was via piston flow. Symmetrical BTCs (Fig. 7) indicate migration of a fairly uniform tracer front through homogeneous material, whereas

Fig. 8. Observed and predicted Cl^- BTCs for control, continuous and discontinuous macropore columns: Column A 0.1 m (a); Column B 0.1 m (b); Column C 0.1 m (c); Column A 0.2 m (d); Column B 0.2 m (e); Column C 0.2 m (f); Column A 0.3 m (g); Column B 0.3 m (h); Column C 0.3 m (i); Column A 0.4 m (j); Column B 0.4 m (k); Column C 0.4 m (l); Column A 0.5 m (m); Column B 0.5 m (n); Column C 0.5 m (o); Column A effluent (p); Column B effluent (q); Column C effluent (r). Pore volumes are defined as in Fig. 6.

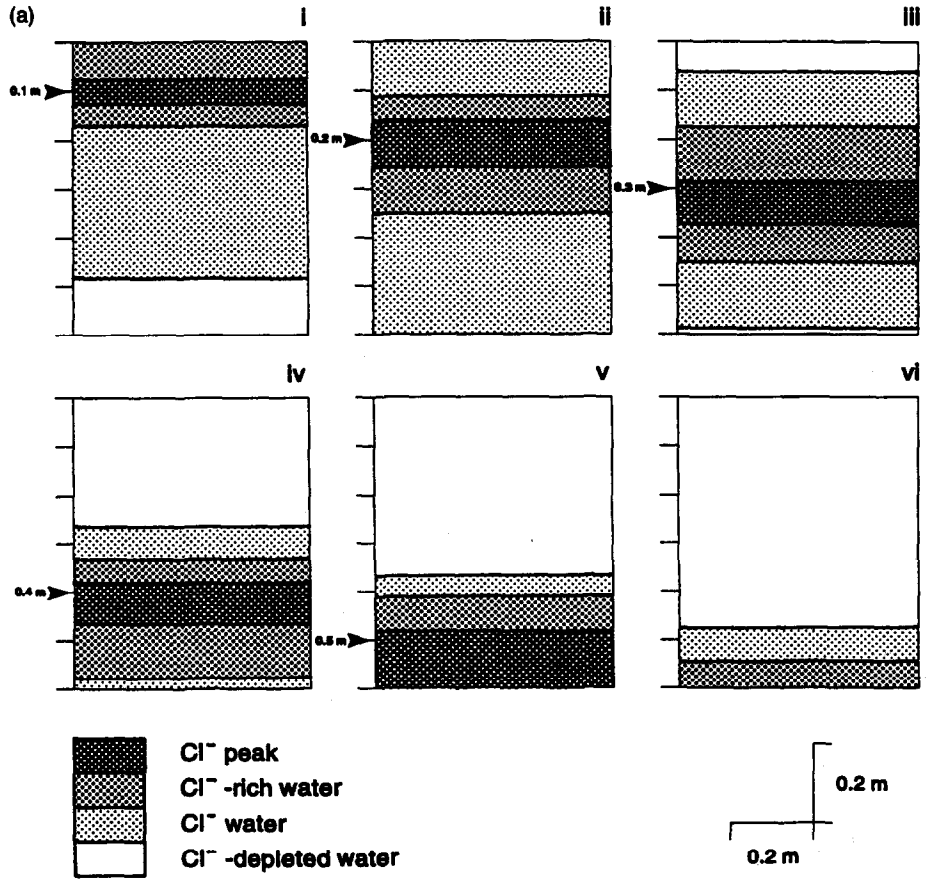

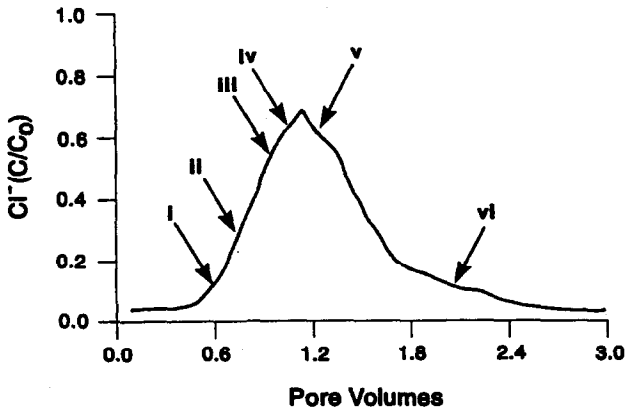

Fig. 9. Conceptual models of Cl^- transport in Column A (a), Column B (b), and Column C (c) Pore volumes are for the entire column.

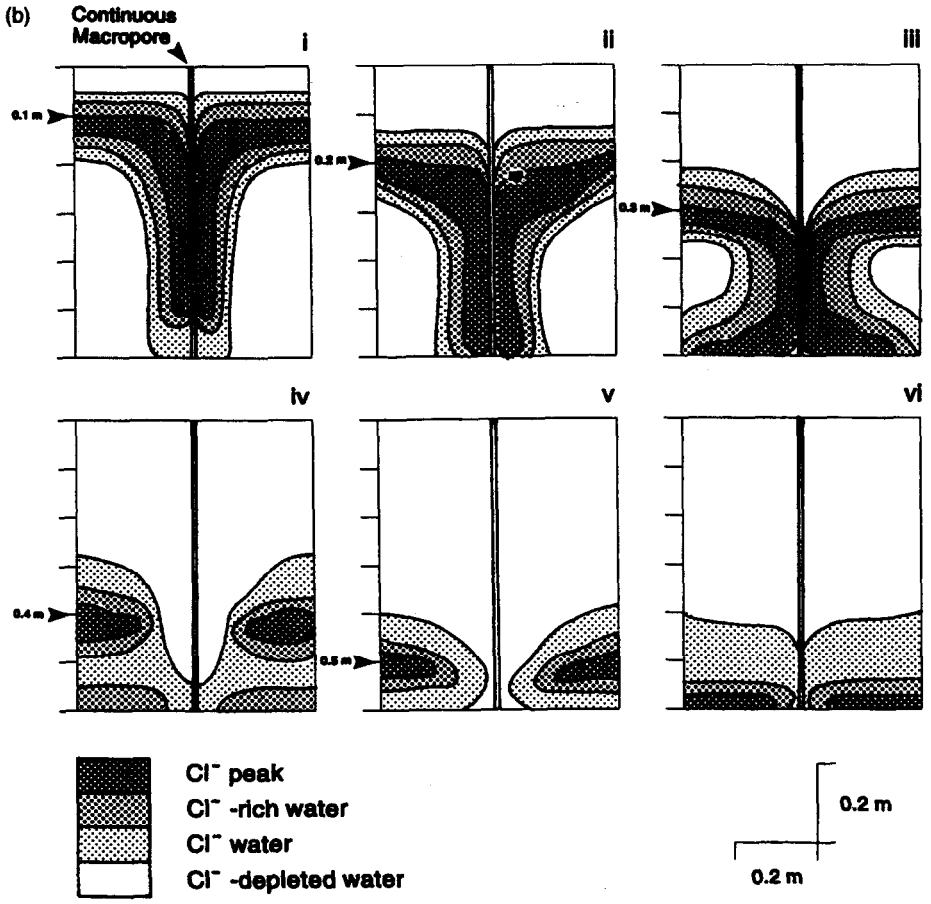

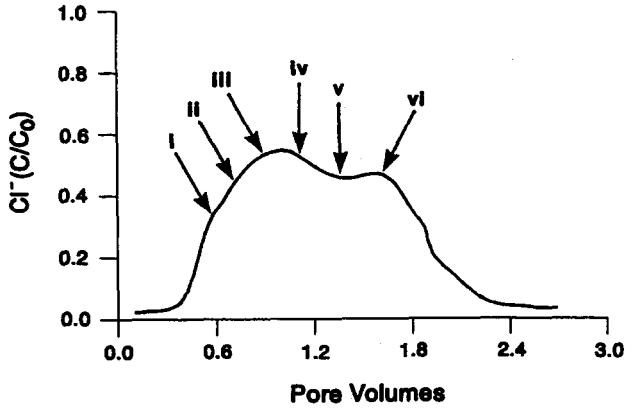

Fig. 9. Continued.

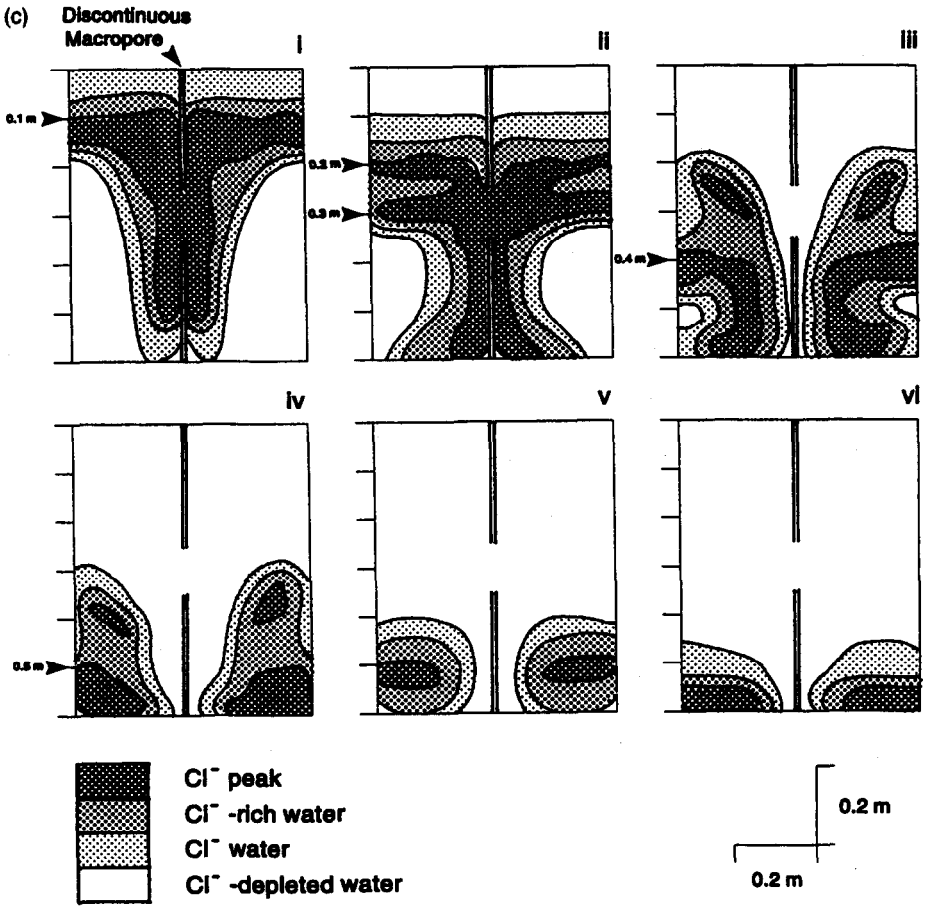

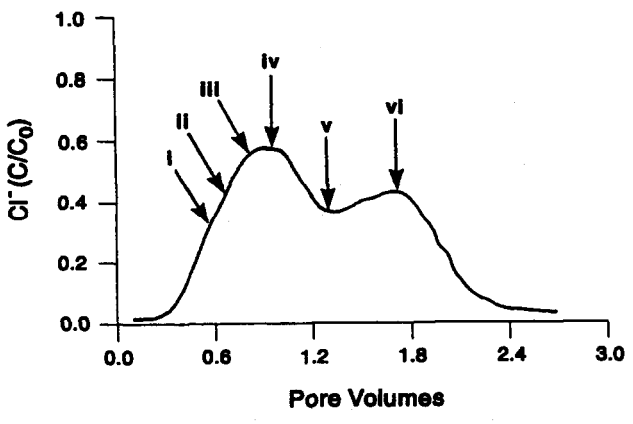

Fig. 9. Continued.

decreasing C/C_0 peaks with depth resulted from Cl^- retention in micropores, increasing dispersion and dilution by resident Cl^--depleted water.

Tracer entered macro- and micropores at the soil surface in Column B (Fig. 9(b)), migrating rapidly to depth while undergoing lateral flow away from the macropore (Edwards et al., 1979; Beven and Germann, 1982). Thus, peak C/C_0 in column effluent was observed whereas the peak C/C_0 in matrix water was about 0.3–0.4 m below the soil surface (Fig. 9(b),iii). Macropore flow limited displacement of matrix water by the tracer application, as suggested by lower θ_m values at given flow lengths relative to Column A (Table 4). These inactive pores may have served as a store of Cl^--depleted water near the column walls. This water gradually mixed with meltwater moving via piston flow through the matrix, producing protracted rising limbs for the 0.4 and 0.5 m suction sampler BTCs (Fig. 7). C/C_0 in column effluent declined as this resident water was displaced and Cl^--depleted water moved down the macropore (Fig. 9(b),v). Additions of Cl^--depleted water to the column displaced Cl^--rich water held in micropores, producing a bimodal effluent BTC. Bimodal tracer BTCs have also been observed in soil column (e.g. Beven and Young, 1988) and field studies (e.g. Starr et al., 1986; Hornberger et al., 1991), and may result from the asynchronous movement of tracer fronts in macro- and micropores observed here.

Water entry to Column C was comparable with that of Column B, as suggested by similar BTCs in near-surface suction samplers (Fig. 7). Macropore flow is hypothesized to have 'backed up' or ponded upon reaching the discontinuity between 0.25 and 0.35 m below the soil surface. This led to enhanced lateral flow away from the macropore, promoting faster Cl^- breakthrough in suction samples at depth than was observed in Column B (Table 3). Simultaneous peak C/C_0 values were observed at the 0.2 and 0.3 m suction samplers (Fig. 7, Fig. 9(c),ii); this may reflect vertical migration of the tracer front in the matrix (0.2 m) and internal catchment (0.3 m). The discontinuity also reduced the flux of Cl^--rich meltwater to the column base early in the experiment, consistent with the smaller number of p.v.s required to reach effluent $C/C_0 = 0.3$ for Column B relative to Column C. Nevertheless, meltwater transport via the discontinuous macropore resulted in faster Cl^- breakthrough in column effluent compared with the control. Internal catchment of Cl^--depleted water contributions separated the Cl^--rich meltwater into two tracer fronts (Fig. 9(c),iii). Dilute water bypassed the macropore discontinuity, displacing Cl^--rich water deeper into the column and producing simultaneous peak C/C_0 values for the 0.5 m suction sampler and column effluent. Effluent C/C_0 declined as Cl^--depleted resident and applied water was displaced from the column (Fig. 9(c),v); however, the decline was more pronounced than in Column B. A second peak in the effluent BTC occurred as the remaining Cl^--rich meltwater was displaced. The difference between the two peak C/C_0 values was greater than in Column B, suggesting that internal catchment of Cl^--depleted water additions resulted in relatively greater dilution of meltwater moving via piston flow through the soil micropores.

4. Conclusions

Use of artificial macropores in a standardized soil under controlled conditions has shown that relatively small (2 mm) macropores have a measurable effect on a soil's

hydraulic properties. Continuous and discontinuous macropores enhanced solute transport, decreased the soil's mobile water content, and increased soil dispersivity. This indicates that the threshold ratio of macropore to micropore diameters required to initiate significant bypassing flow in soils is less than that presented by Kirkby (1988). Such ratios provide only a partial means of identifying potential for bypassing flow, and Edwards et al. (1993) suggested that the threshold ratio for bypassing will vary in response to such factors as the rate and amount of infiltration.

Macropores with diameters of the order of 2 mm dominate the macroporosity of some soils (Ehlers, 1975; Edwards et al., 1993). Larger macropores serve as more efficient conduits of preferential flow by virtue of their greater diameters; however, smaller macropores would probably fill with water and begin to conduct flow during rainfall or snowmelt before preferential flow could be generated in larger macropores. In addition, large macropores may not conduct flow during relatively small additions of water to the soil surface, whereas smaller macropores may still serve as preferential pathways under these conditions (cf. Thomas et al., 1978). Thus, studies of relatively large macropores (i.e. greater than 5 mm diameter) may underestimate the occurrence of preferential flow in soils.

Bimodal effluent BTCs were observed for columns containing continuous and discontinuous macropores, and there was little difference in breakthrough times for the two macropore types. Flow was apparently able to pass quickly through the 0.1 m discontinuity and reach the base of Column C. The transport efficiency of small and discontinuous macropores shown in this and other studies (e.g. Phillips et al., 1989) calls into question the effectiveness of agricultural practices that aim to reduce leaching of agrochemicals by severing large continuous macropores close to the soil surface.

Use of artificial macropores under controlled conditions may provide useful information on the role of macropores in solute transport through soils. Future work should incorporate such laboratory studies with field and modelling investigations of macropore flow.

Acknowledgements

This work was funded through a grant from the Natural Sciences and Engineering Research Council of Canada.

References

Anderson, S.H., Peyton, R.L. and Gantzer, C.J., 1990. Evaluation of constructed and natural soil macropores using x-ray computed tomography. Geoderma, 46: 13–29.

Beven, K.J. and Germann, P.F., 1982. Macropores and water flow in soils. Water Resour. Res., 18: 1311–1325.

Beven, K.J. and Young, P.C., 1988. An aggregated mixing zone model of solute transport through porous media. J. Contam. Hydrol., 3: 129–143.

Booltink, H.W.G., 1994. Field-scale distributed modelling of bypass flow in a heavily textured clay soil. J. Hydrol., 163: 65–84.

Bouma, J., 1990. Using morphometric expressions for macropores to improve soil physical analyses of field studies. Geoderma, 46: 3–11.

Bouma, J. and Anderson, J.L., 1977. Water and chloride movement through soil columns simulating pedal soils. Soil Sci. Soc. Am. J., 41: 766–770.

Buttle, J.M., 1989. Soil moisture and groundwater responses to snowmelt on a drumlin sideslope. J. Hydrol., 105: 335–355.

Chen, C. and Wagenet, R.J., 1992. Simulation of water and chemicals in macropore soils, Part 1. Representation of the equivalent macropore influence and its effect on soilwater flow. J. Hydrol., 130: 105–126.

Czapar, G.F., Horton, R. and Fawcett, R.S., 1992. Herbicide and tracer movement in soil columns containing an artificial macropore. J. Environ. Qual., 21: 110–115.

Davidson, D.A., 1978. Science for Physical Geographers. Edward Arnold, London, 187 pp.

De Smedt, F., Wauters, F. and Sevilla, J., 1986. Study of tracer movement through unsaturated sand. J. Hydrol., 85: 169–181.

Dingman, S.L., 1993. Physical Hydrology. Prentice–Hall, Englewood Cliffs, NJ, 575 pp.

Drever, J.I., 1988. The Geochemistry of Natural Waters. Prentice–Hall, Englewood Cliffs, NJ, 437 pp.

Edwards, W.M., van der Ploeg, R.R. and Ehlers, W., 1979. A numerical study of the effects of non-capillary sized pores upon infiltration. Soil Sci. Soc. Am. J., 43: 851–856.

Edwards, W.M., Shipitalo, M.J., Owens, L.B. and Dick, W.A., 1993. Factors affecting preferential flow of water and atrazine through earthworm burrows under continuous no-till corn. J. Environ. Qual., 22: 453–457.

Ehlers, W., 1975. Observations on earthworm channels and infiltration on tilled and untilled loess soil. Soil Sci., 119: 242–248.

Elrick, D.E. and French, L.K., 1966. Miscible displacement patterns on disturbed and undisturbed soil cores. Soil Sci. Soc. Am. Proc., 30: 153–156.

Fetter, C.W., 1994. Applied Hydrogeology, 3rd edn. Macmillan, London, 691 pp.

Flury, M., Fluhler, H., Jury, W.A. and Leuenberger, J., 1994. Susceptibility of soils to preferential flow of water: a field study. Water Resour. Res., 30: 1945–1954.

Germann, P.F., 1991. Length scales of convection–dispersion approaches to flow and transport in porous media. J. Contam. Hydrol., 7: 39–49.

Germann, P.F. and Beven, K.J., 1986. A distribution function approach to water flow in soil macropores based on kinematic wave theory. J. Hydrol., 83: 173–183.

Hornberger, G.M., Germann, P.F. and Beven, K.J., 1991. Throughflow and solute transport in an isolated sloping soil block in a forested catchment. J. Hydrol., 124: 81–89.

Jardine, P.M., Wilson, G.V., Luxmoore, R.J. and McCarthy, J.F., 1989. Transport of inorganic and natural organic tracers through an isolated pedon in a forest watershed. Soil Sci. Soc. Am. J., 53: 317–323.

Jarvis, N.J., Bergstrom, L. and Dik, P.E., 1991. Modelling water and solute transport in macroporous soil. II. Chloride breakthrough under non-steady flow. J. Soil Sci., 42: 71–81.

Jones, L.A., Rutledge, E.M., Scott, H.D., Wolf, D.C. and Teppen, B.J., 1993. Effects of two earthworm species on movement of septic tank effluent through soil columns. J. Environ. Qual., 22: 52–57.

Kirkby, M.J., 1988. Hillslope runoff processes and models. J. Hydrol., 100: 315–339.

Kluitenberg, G.J. and Horton, R., 1990. Effect of solute application method on preferential transport of solutes in soil. Geoderma, 46: 283–297.

Leigh, D.G., 1995. Isotopic and chemical tracing of macropore flow in laboratory soil columns under simulated snowmelt conditions. M.Sc. Thesis, Watershed Ecosystems Graduate Program, Trent University, Peterborough, Ont., 166 pp.

Luxmoore, R.J., 1981. Micro-, meso-, and macroporosity of soil. Soil Sci. Soc. Am. J., 45: 671.

McMahon, M.A. and Thomas, G.W., 1974. Chloride and tritiated water flow in disturbed and undisturbed soil cores. Soil Sci. Soc. Am. Proc., 38: 727–732.

Munyankusi, E., Gupta, S.E., Moncrief, J.F. and Berry, E.C., 1994. Earthworm macropores and preferential transport in a long-term manure applied Typic Hapludalf. J. Environ. Qual., 23: 773–784.

Neuman, S.P., 1990. Universal scaling of hydraulic conductivities and dispersivities in geologic media. Water Resour. Res., 26: 1749–1758.

Nielsen, D.R., van Genuchten, M.Th. and Biggar, J.W., 1986. Water flow and solute transport processes in the unsaturated zone. Water Resour. Res., 22: 89S–108S.

Phillips, R.E., Quisenberry, V.L., Zeleznik, J.M. and Dunn, G.H., 1989. Mechanisms of water entry into simulated macropores. Soil Sci. Soc. Am. J., 53: 1629–1635.

Quisenberry, V.L. and Phillips, R.E., 1978. Displacement of soil water by simulated rainfall. Soil Sci. Soc. Am. J., 42: 675–679.